

A Crusher Gradient Scheme for Stimulated Echo Double Wave Vector Diffusion Imaging for 7T Human MRI

Grant Kaijuin Yang^{1,2}, Christoph W.U. Leuze², and Jennifer McNab²

¹Electrical Engineering, Stanford University, Stanford, California, United States, ²Radiology, Stanford University, Stanford, California, United States

Target Audience: Physicists, neuroscientists and clinicians who are interested in studying tissue microstructure through diffusion imaging.

Introduction: Double Wave Vector (DWV) imaging¹ provides additional information about tissue microstructure not available through conventional diffusion imaging including markers of compartment shape, size, and orientation^{1,2,3,4}. DWV extends the classic Stejskal-Tanner diffusion sequence by appending a second diffusion-encoding pair of gradients (Fig. 1: G₂). For angular-DWV imaging, restricted diffusion effects are encoded through multiple measurements acquired with different angles between the orientations of G₁ and G₂ (Fig. 1). Stimulated echo (STE) based angular-DWV sequences may provide a significant improvement in SNR compared to spin echo (SE) for long mixing and diffusion times and/or short T₂ species³. In addition, the 90° pulses used in STE sequences are less SAR intensive and easier to execute accurately at high field compared to the 180° pulses used in SE sequences. However, the use of DWV sequences on clinical systems has primarily been limited to SE versions due to complications with echo pathway selection presented by the additional RF pulses in a STE sequence. These spurious echoes are particularly problematic in wide-bore, high field clinical scanners due to increased B₁ and B₀ inhomogeneities. As such, adapting STE-DWV sequences from NMR to MRI is non-trivial. We present a crusher gradient scheme to address spurious echo artifacts in STE-DWV on a human 7T MRI.

Theory: A gradient scheme was designed to suppress unwanted coherence pathways by dephasing all magnetization pathways except the STE formed by the first and last three RF pulses⁵. To form the STE, the transverse crusher pairs (Fig. 1: G_{crush-z}) must have equal area, while all other crusher combinations must induce at least one cycle of phase/voxel to avoid spurious echo formation. This constraint was simplified by applying the longitudinal period crushers (Fig.

1: G_{crush-y}) along a different axis than the transverse crushers to avoid undesired rephasing between the transverse and longitudinal crushers. In the first experiment the transverse gradient areas were chosen to induce [2,2,4,4] cycles of phase per voxel, and the longitudinal crushers were chosen to induce [8,6,10] cycles of phase per voxel. Since the longitudinal period crushers do not affect the diffusion weighting of the resulting signal, the crusher area could be chosen to be conservatively large. The crusher scheme allows T₁ relaxation during the mixing time to contribute to the signal. This contribution could be removed by altering the transverse crusher areas to only produce the final STE [2,4,3,1], but it would result in the loss of half the signal as the first stimulated echo would not be refocused when the fourth RF pulse is applied. Of note, the signal contribution from T₁ relaxation during t_m is estimated to be significant for the short T₁,T₂ species of the silicon phantom used in this study (~74%), however, this effect is minimal (~3-5%) for the longer T₁,T₂ species typical of *in vivo* human brain and not expected to change our evaluation of the crusher scheme.

Methods: The crusher scheme was tested on a 7T GE MR950 whole-body scanner (G_{max}= 50 mT/m and a SR=200 T/m/s) with a 32 channel Nova head coil using a dimethyl silicon spherical phantom with T₁/T₂ = 190/17 ms and relative immunity to B₁ inhomogeneities. The parameters for the STE-DWV sequence (Fig. 1) were TE/TR = 100/1000ms, 20cmx20cm FOV, 64x64 matrix, BW=±62.5 kHz and 5 mm slice thickness. The diffusion parameters were Δ = 50 ms, δ = 20 ms, t_m = 45 ms and G_{diff}=50 mT/m for a b-value of 315 s/mm² for each diffusion encoding direction. The first diffusion direction was applied on the logical x-axis, while the second gradient direction was rotated in 90° increments in the slice plane. Phase cycling⁶ was also applied but found to have little effect on the appearance of image artifacts. This resulted in a total scan time of 34 minutes.

Results and Discussion: As seen in Fig. 2, the STE sequence produces significant image artifacts when the diffusion gradients are parallel or antiparallel. This induces not only visible stripes in the image, but also additional variations in signal intensity (Fig. 3), which could obscure the restricted diffusion effects. The artifacts increase when G₁ and G₂ are applied along the same direction, because undesired echo pathways can form due to refocusing between G₁ and G₂. This interference is completely suppressed by the proposed crusher scheme, resulting in the expected flat signal response for free diffusion.

Conclusions: The crusher gradient scheme successfully suppressed artifacts and signal variations from unwanted coherence pathways in the STE-DWV sequence. Therefore, the crusher scheme designed and demonstrated here represents a significant step towards the translation of DWV measurements to whole body high field scanners where the additional information about tissue microstructure revealed by DWV imaging could be applied to basic neuroscience and clinical applications.

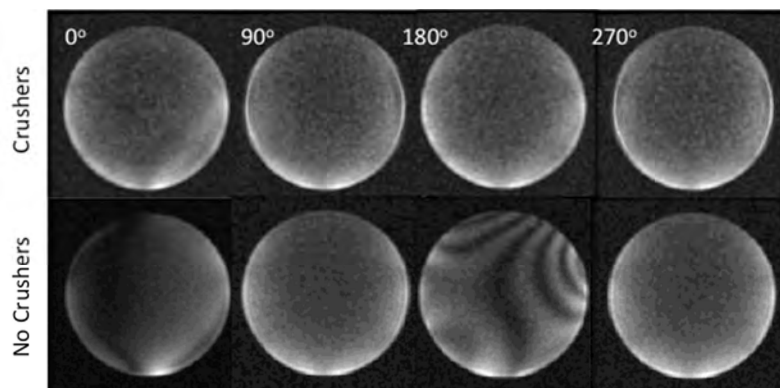


Figure 2: Silicon-based phantom showing artifacts (bottom) when no crushers are applied, and an artifact free image (top) with the proposed crusher scheme.

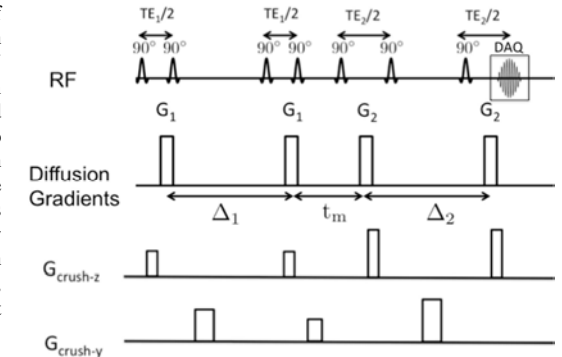


Figure 1: Stimulated echo DWV pulse sequence showing proposed crusher scheme and diffusion gradients. Imaging gradients have been neglected in this diagram.

10
5
0
-5
-10

With Crushers
Without Crushers

100 150 200 250

0 50 100 150 200 250

% Signal Fluctuation

ψ (°)

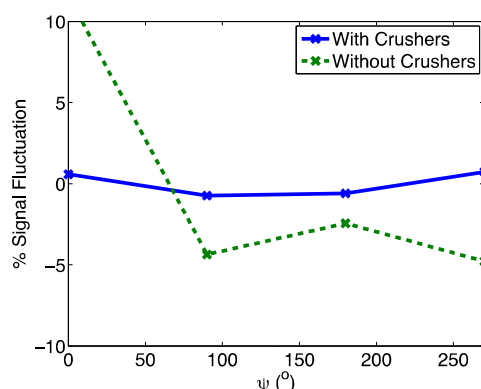


Figure 3: Percent signal fluctuation versus the angle between G₁ and G₂ (ψ).

Acknowledgments: Funding for this work was provided by an NSF-GRFP, a Li Ka Shing-Oxford-Stanford Big Data in Human Health Seed grant, NIH: S10-RR026351, P41-EB015891, Stanford Radiology Angel Funds, and GE Healthcare. Thanks for helpful discussions from Professors John Pauly, Brian Hargreaves, and Brian Rutt.

References: [1] Mitra APS 51(21) 15074-15078, 1995. [2] Koch et. al. MRM, 60, 90-101, 2008. [3] Shemesh et al. MRM, 65, 1216-1227, 2011. [4] Ozarslan et al. JCP. 130, 104702, 2009. [5] Bernstein ISBN: 978-0-12-092861-3. [6] Khrapitchev et. a. JMR, 29(9), 259-268, 2001.